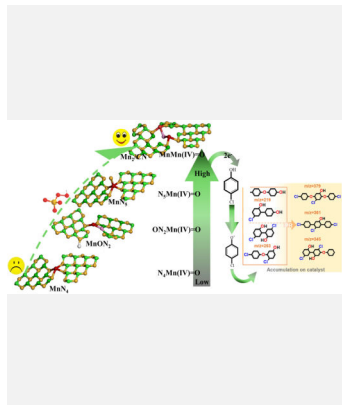


Mingce Long<sup>1\*</sup>, Bo He<sup>1</sup>, Jie Miao<sup>1</sup>, Pedro J. J. Alvarez<sup>2</sup>. (1) Shanghai Jiao Tong University, 800 Dongchuan Road, Shanghai, China, long\_mc@sjtu.edu.cn. (2) Rice University, 6100 Main Street, Houston, United States



In peroxymonosulfate (PMS)-based advanced oxidation processes (AOPs), stable and efficient functional materials are the crucial. Single-atom catalysts (SACs) are broadly recognized as the most efficient active sites, but diatomic catalyst and SACs with a coordination number higher than four are rarely explored. We experimentally demonstrate here that five-nitrogen-coordinated Mn ( $MnN_5$ ) and diatomic Mn ( $Mn_2/CN$ ) more effectively activate PMS than  $MnN_4$  sites. The high activity of  $MnN_5$  was discerned to be due to the formation of higher-spin-state  $Mn^{IV}=O$ , which enable efficient two-electron transfer from organics to Mn sites. The interaction between the coordination of Mn DACs and their electronic structures may provide a more optimized structure, which is beneficial for the adsorption and desorption of substrates to reach appropriate states and improve intrinsic activity. Overall, this work aims to develop efficient manganese catalysts at the molecular level for PMS-based AOPs.

## Introduction

Heterogeneous peroxymonosulfate (PMS)-based advanced oxidation processes (AOPs) are powerful remediation technologies to treat recalcitrant organic contaminants in water. High-valent metal-oxo (HVMO) species, as typical nonradical oxidative species generated in persulfate activation, are promising candidates for water purification, owing to their much longer lifetime higher steady-state concentrations, ultrahigh oxidant utilization efficiency, and selective reactivity toward organics. However, HVMO species are usually generated in homogeneous systems catalyzed by transition metals that also produce other reactive species, and this decreases the utilization efficiency of the oxidant. Therefore, it is important to develop transition metal-based heterogeneous catalysts that activate persulfate by efficiently generating HVMO species with high reactivity.

We experimentally and theoretically investigated the five-nitrogen coordinated Mn configuration ( $MnN_5$ ) and diatomic Mn ( $Mn_2/CN$ ) in PMS activation via the Mn–HVMO pathway. We synthesized  $MnN_5/CN$  and  $Mn_2/CN$  to demonstrate the importance of high coordination numbers and electronic structure for efficient PMS activation. This work provides information for the design of next-generation catalysts.

## Material and Methods

**Materials.** Dicyandiamide (DCD), manganese(III) acetylacetonate ( $Mn(acac)_3$ ), ammonium chloride ( $NH_4Cl$ ), PMS, and were purchased from Sigma-Aldrich Chemical Co., Ltd. Manganese(II) chloride ( $MnCl_2$ ), oxalic acid, and 2,2'-bipyridine were obtained from Sinopharm Chemical Reagent Co., Ltd.

**Synthesis of g-C<sub>3</sub>N<sub>4</sub>.** The DCD was heated to 550 °C with a rate of 2.5 °C/min and kept for 4 h in a muffle furnace.

**Synthesis of  $Mn_2(bpy)_2(\mu-ox)$ .** The copper-dimer precursor  $Mn_2(bpy)_2(\mu-ox)$  was first prepared by a complexation reaction of manganese chloride ( $MnCl_2$ ), 2,2'-bipyridine and oxalic acid.

**Synthesis of Mn SACs.** For the synthesis of  $MnN_5$ ,  $NH_4Cl$  was selected to control the coordination environment of Mn single-atom sites on g-C<sub>3</sub>N<sub>4</sub>. Typically, g-C<sub>3</sub>N<sub>4</sub> and  $Mn(acac)_3$  were mixed with  $NH_4Cl$  molar weight in a mortar and thoroughly grinded. Then, the obtained sample was heated to 550 °C with a rate of 2.5 °C/min under an Ar atmosphere for 4 h in a tube furnace.  $MnN_4$  was synthesized by a similar procedure but without the addition of  $NH_4Cl$ .

**Synthesis of  $Mn_2/CN$ .** The only difference between  $MnN_5$  and  $Mn_2/CN$  is that the precursor  $Mn_2(bpy)_2(\mu-ox)$  is chosen.

## Results and Discussion

Atomic structures of the dimeric manganese moieties were resolved by using aberration correction high angle annular dark field scanning transmission electron microscopy (HAADF-STEM) imaging (Fig. 1a). The collected STEM images exhibit a large number of adjacent, paired bright dots (labeled with red circles, <0.35 nm in size for each dot) distributed on a substrate of lower contrasts. These small bright dots can be attributed to atomically dispersed Cu considering their much higher Z contrast than C<sub>3</sub>N<sub>4</sub>. Line-profile scanning for 33 pairs of such bright dots give an average distance of 2.7 (±0.07 Å) (Fig. 1b). This is much shorter than the value (5.2 Å) for the two manganese atoms within  $Mn_2(bpy)_2(\mu-ox)$ , again confirming the reconstruction

and condensation of the manganese-dimer moieties as a result of the removal of organic ligands in the synthesis.

In the in situ Raman spectra of PMS (Fig. 1c), the simultaneous appearance of a new Raman peak at  $751\text{ cm}^{-1}$  could be assigned to the stretching vibration of  $\text{Mn}^{\text{IV}}\text{-oxo}$  structures, suggesting that PMS molecules chemically bound to  $\text{Mn}_2/\text{CN}$  sites dissociated and transformed into  $\text{Mn}^{\text{IV}}\text{-oxo}$  species<sup>[2]</sup>. Similar phenomena were also observed in the  $\text{MnN}_5/\text{PMS}$  system, indicating that PMS activation pathways over the two catalysts were similar. Furthermore, the  $\text{Mn}^{\text{IV}}\text{-oxo}$  stretching frequency ( $751\text{ cm}^{-1}$ ), persisting under ambient conditions, disappeared immediately after the addition of 4-CP, implying that  $\text{Mn}^{\text{IV}}\text{-oxo}$  species have a strong oxidation capacity to induce a rapid electron transfer from 4-CP to  $\text{Mn}^{\text{IV}}\text{-oxo}$ .

We then conducted density functional theory (DFT) calculations to explore PMS adsorption and activation over Mn SACs. On the surface of two catalysts, PMS is chemically bound to the Mn sites by one peroxy oxygen in a terminal end-on mode with large adsorption energies. The longer O-O bond on  $\text{MnN}_5$  suggests a higher PMS activation capacity. The charge density difference mappings corroborate enhanced PMS activation on  $\text{MnN}_5$  because more electrons are delocalized from Mn atoms to the bounded oxygen of  $\text{MnN}_5$  than that of  $\text{MnN}_4$ . Thus, we estimated that a Mn SAC with five-nitrogen coordination is an efficient catalyst for PMS activation, which is consistent with the experimental results.

The enhanced reactivity of  $\text{Mn}^{\text{IV}}\text{-o}$  was corroborated by in situ open-circuit potential (OCP) tests via recording OCP values of Mn SAC and DAC electrodes with the increase of PMS dosages. The  $\text{Mn}_2/\text{CN}$  and  $\text{MnN}_5$  electrode had the highest positive OCP value in the  $\text{MnN}_4$ , suggesting that the  $\text{Mn}^{\text{IV}}\text{-o}$  species of  $\text{Mn}_2/\text{CN}$  and  $\text{MnN}_5$  have the highest

## Conclusions

Mn DACs and five-nitrogen coordinated Mn SACs are efficient catalyst for the treatment of wastewater contaminated by recalcitrant organic compounds and for groundwater remediation by PMS-based AOPs. This work addresses the fundamental knowledge gap in promoting PMS activation in coordination chemistry and emphasizes the key reason why  $\text{Mn}_2/\text{CN}$  and  $\text{MnN}_5$  forms highly active  $\text{Mn}^{\text{IV}}\text{-o}$  species. Specifically, during PMS activation, Mn(II) sites on the catalysts are spontaneously oxidized into reactive  $\text{Mn}^{\text{IV}}\text{-o}$  species, whose reactivity strongly depends on the coordination number of nitrogen atoms and the electronic structure of Mn. These mechanistic insights suggest that the activity of SAC in HVMO mediated PMS activation depends not only on the coordination number that controls the reactivity of HVMO species, but also on the electronic regulation between metal atoms. Overall, this work provides a strategy for developing DACs and SACs with high nitrogen coordination numbers, which can enhance PMS-based AOPs for developing next-generation environmental catalysts and enhancing HVMO-mediated PMS based AOPs.

## Acknowledgments

Financial supports from the National Natural Science Foundation of China (nos. 22376138, 52070128) are gratefully acknowledged.

## References

- [1] Z. Wang, S. Pang, W. Qiu, Q. Guo, C. Guan, J. Jiang, Environ. Sci. Technol. 56 (2022) 1492.
- [2] M. Guo, M. Sookseo, Y. Minlee, S. Fukuzumi, W. Nam, J. Am. Chem. Soc., 141 (2019) 12187.
- [3] M. Jie, S. Jian, L. Junyu, L. Mingce, S. Zongping, Z. Baoxue, A. Pedro J.J, Environ. Sci. Technol. 57 (2023) 4266.

oxidative capacity. We normalized the positive potential difference ( $\Delta E$ ) values by the unit moles of catalysts to obtain a parameter ( $\Delta E_{\text{per-site}}$ ). A linear positive correlation between  $\Delta E_{\text{per-site}}$  and  $k_{\text{per-site-4-CP}}$  ( $R^2 \geq 0.75$ ) was obtained. The slope of the correlation curve, representing the increased tendency of the organic degradation rate at the same increase of  $\Delta E_{\text{per-site}}$  for Mn SACs and DACs, is an indicator of the intrinsic reactivity of  $\text{Mn}^{\text{IV}}\text{-O}$  species generated in PMS activation. The slope value in the  $\text{Mn}_2/\text{CN} / \text{PMS}$  system was 3.55, significantly higher than that of Mn SAC (0.43), further proving the significantly enhanced intrinsic reactivity of  $\text{Mn}^{\text{IV}}\text{-o}$  species in the  $\text{Mn}_2/\text{CN}$  (Fig. 1d)<sup>[3]</sup>. The  $k_{\text{SA}}$  value of  $\text{Mn}_2/\text{CN}$  ( $0.151\text{ min}^{-1}\text{ g m}^{-2}$ ) and  $\text{MnN}_5$  ( $0.022\text{ min}^{-1}\text{ g m}^{-2}$ ) were highest, and higher than that of  $\text{g-C}_3\text{N}_4$  ( $0.0002\text{ min}^{-1}\text{ g m}^{-2}$ ) and  $\text{MnN}_4$  ( $0.006\text{ min}^{-1}\text{ g m}^{-2}$ ), respectively. The intrinsic catalytic performance of  $\text{Mn}_2/\text{CN}$  and  $\text{MnN}_5$  were superior to that of many reported Mn-based catalysts and Cu/Fe SACs (Fig. 1e).

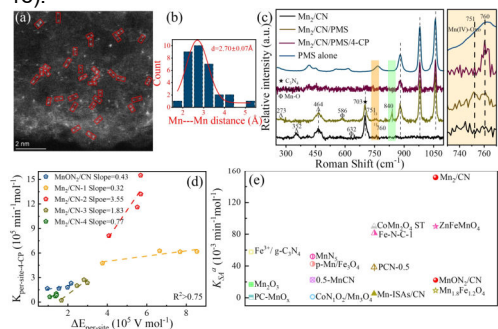


**Figure 1.** (a) Representative HAADF-STEM images of  $\text{Mn}_2/\text{CN}$ . (b) Statistical distribution of the Mn-Mn distance. (c) In situ Raman spectra. (d) Relationship between specific potential changes ( $\Delta E_{\text{SSA}}$ ) and  $k_{\text{SA}}$  for 4-CP degradation. (e) Comparison of the kinetics of organic pollutants degradation in the reported heterogeneous PMS-based AOPs.